

UNCLASSIFIED

AD NUMBER
ADB182385
NEW LIMITATION CHANGE
TO Approved for public release, distribution unlimited
FROM Distribution authorized to U.S. Gov't. agencies and their contractors; Administrative/Operational Use; 12 AUG 1960. Other requests shall be referred to National Aeronautics and Space Administration, Washington, DC.
AUTHORITY
NASA TR Server Website

THIS PAGE IS UNCLASSIFIED

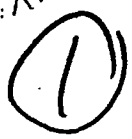
AD-B182 385



ms. Robert L. Page 54

d.k.

COPY 1



8670

N-86782

GEORGE C. MARSHALL

SPACE
FLIGHT
CENTER

HUNTSVILLE, ALABAMA

S DTIC
ELECTE
FEB 22 1994
A

LIBRARY COPY

AUG 29 1960

August 12, 1960

AN ANALYSIS OF THE THERMODYNAMIC CYCLE
AND POSSIBLE WORKING FLUIDS FOR A
SPACE HEAT REJECTION SYSTEM

By George C. Bucher

3/PS

94-05477

"DTIC USERS ONLY"



NATIONAL AERONAUTICS AND SPACE ADMINISTRATION

04-2 18 069

DTIC QUALITY INSPECTED &

August 12, 1960

MNN-M-RP-5-60

**AN ANALYSIS OF THE THERMODYNAMIC CYCLE AND
POSSIBLE WORKING FLUIDS FOR A
SPACE HEAT REJECTION SYSTEM**

by

George C. Bucher

Accession For	
NTIS CRA&I	<input type="checkbox"/>
DTIC TAB	<input checked="" type="checkbox"/>
Unannounced	<input type="checkbox"/>
Justification	
By	
Distribution/	
Availability Codes	
Dist	Avail and/or Special
12	

"DTIC USERS ONLY"

**TECHNICAL AND SCIENTIFIC ASSISTANT
RESEARCH PROJECTS DIVISION**

ABSTRACT

Within the next few years, nuclear reactor - thermal systems will most logically supply the large power requirements for space vehicles utilizing electric propulsion units. An integral part of the system is the radiator for the dissipation of waste heat.

The ideal Carnot thermodynamic cycle is analyzed to determine the relationship between radiator characteristics and the over-all system. For minimum radiator area, the heat rejection temperature is shown to be three-fourths of the heat addition temperature. An expression is derived for minimum radiator area as a function of power output of the cycle and radiator temperature, and the Carnot cycle efficiency is shown to be 25 percent for minimum radiator area. The analysis is then extended to the actual Rankine thermodynamic cycle, taking into account properties of working fluids and the inefficiencies of system components. An expression is derived to show the relationship between the radiator temperature and heat addition temperature for the case of optimum cycle work and minimum radiator area. Another equation expresses the radiator area as a function of power output and the heat addition and heat rejection temperatures of the actual Rankine cycle. A figure illustrates that increased heat addition temperatures result in substantial reductions in the radiator size.

Suitable working fluids for a nuclear reactor - thermal system are discussed. Elements are more attractive than alloys or compounds. Liquid metals have desirable properties; rubidium, potassium and sodium are found to be most suitable for the system described.

TABLE OF CONTENTS

	Page
ABSTRACT	ii
LIST OF SYMBOLS	iv
1. INTRODUCTION	1
2. CYCLE ANALYSIS TO DETERMINE RADIATOR CHARACTERISTICS	1
a. Ideal Carnot Cycle	3
b. Actual Rankine Cycle	6
3. WORKING FLUIDS	15
REFERENCES	24

LIST OF SYMBOLS

Q_R	heat radiated
Q_A	heat added
σ	Stefan-Boltzmann constant
ϵ	emissivity
A_R	area of radiator
S	entropy
h	enthalpy
T_R	temperature of radiator
T_A	heat addition temperature
W_C	work of Carnot cycle
W_R	work of actual Rankine cycle
k	work factor
η_C	efficiency of Carnot cycle
η_t	efficiency of turbine
η_r	efficiency of actual Rankine cycle

1. INTRODUCTION

Space vehicles utilizing electric propulsion units will require large amounts of power. Within the next few years the nuclear reactor-thermal system appears to be the most attractive system to meet these requirements.

Mackay [1] has compared thermal powerplant cycles for space vehicles and has concluded that vapor cycles are far superior to other thermal cycles, including the Brayton gas cycle. He found that the efficiencies of the vapor cycles are not greatly different from those obtainable with the ideal Carnot cycle, and therefore are probably the best that can be obtained from a thermal cycle.

In this paper, consideration will be given to a thermodynamic vapor cycle, as may be envisioned for use in a space vehicle. The power, propulsion and heat rejection system is shown schematically in Figure 1. The heat source is a nuclear reactor wherein the liquid working fluid is transformed to a vapor which passes through a turbine and into a radiator where it is condensed back to a liquid, accompanied by a rejection of waste heat. The direct condenser-radiator may not necessarily be the best scheme for condensing vapor in an actual space vehicle, but it is considered feasible.

The purpose of this paper is to present an analysis of the thermodynamic cycle to determine the relationship between the radiator characteristics and the over-all system, and to discuss possible working fluids for a nuclear reactor-thermal system.

2. CYCLE ANALYSIS TO DETERMINE RADIATOR CHARACTERISTICS

The system shown in Figure 1 utilizes an actual Rankine cycle for the working fluid. The Rankine cycle closely approaches the Carnot cycle in principle. The Carnot cycle is considered the ideal thermodynamic cycle. By comparing the performance of the actual Rankine cycle to the Carnot cycle, one may see how near the actual cycle is to perfection.

Therefore, an analysis will first be made of the Carnot cycle to determine the characteristics of the radiator. The analysis will then be extended to the actual Rankine cycle, to determine the radiator characteristics as influenced by an actual (rather than an ideal) working fluid and by inefficiencies of system components.

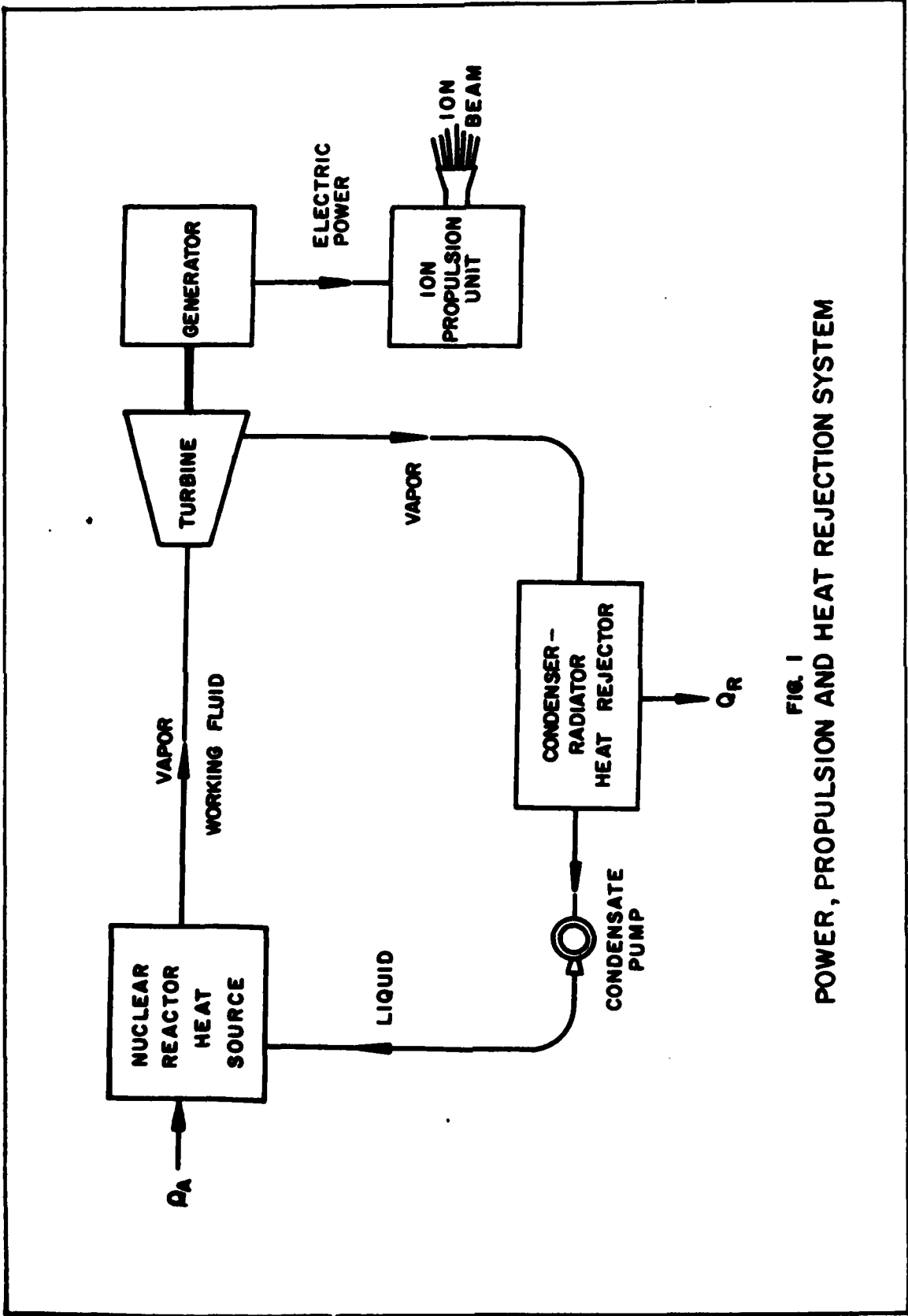


FIG. 1
 POWER, PROPULSION AND HEAT REJECTION SYSTEM

a. Ideal Carnot Cycle

The Carnot cycle is shown in Figure 2. It produces the maximum amount of work obtainable from a heat engine operating between two fixed temperature limits. In this idealized cycle, the working fluid is isentropically compressed between points d and a ; heat is added isothermally at temperature T_A between points a and b ; the fluid is isentropically expanded between points b and c ; and heat is rejected from the fluid isothermally between points c and d . The efficiency of the idealized Carnot cycle is independent of the properties of the working fluid.

Using the temperature - entropy diagram of Figure 2, the efficiency of the cycle is derived by Paires [2] as follows:

$$Q_A = \text{Heat Added} = \text{area under curve a-b}$$

$$= T_A(S_b - S_a)$$

$$Q_R = \text{Heat Rejected} = \text{area under curve c-d}$$

$$= T_R(S_b - S_a)$$

$$W_C = \text{Net work of the Carnot cycle} = Q_A - Q_R$$

$$= T_A(S_b - S_a) - T_R(S_b - S_a)$$

$$= (T_A - T_R)(S_b - S_a)$$

$$\eta_c = \text{Thermal efficiency} = \frac{W_C}{Q_A} = \frac{Q_A - Q_R}{Q_A}$$

$$= \frac{(T_A - T_R)(S_b - S_a)}{T_A(S_b - S_a)} = \frac{T_A - T_R}{T_A} \quad (1)$$

From Eq. (1), the following relationship exists:

$$\frac{W_C}{Q_A} = \frac{T_A - T_R}{T_A} \quad (2)$$

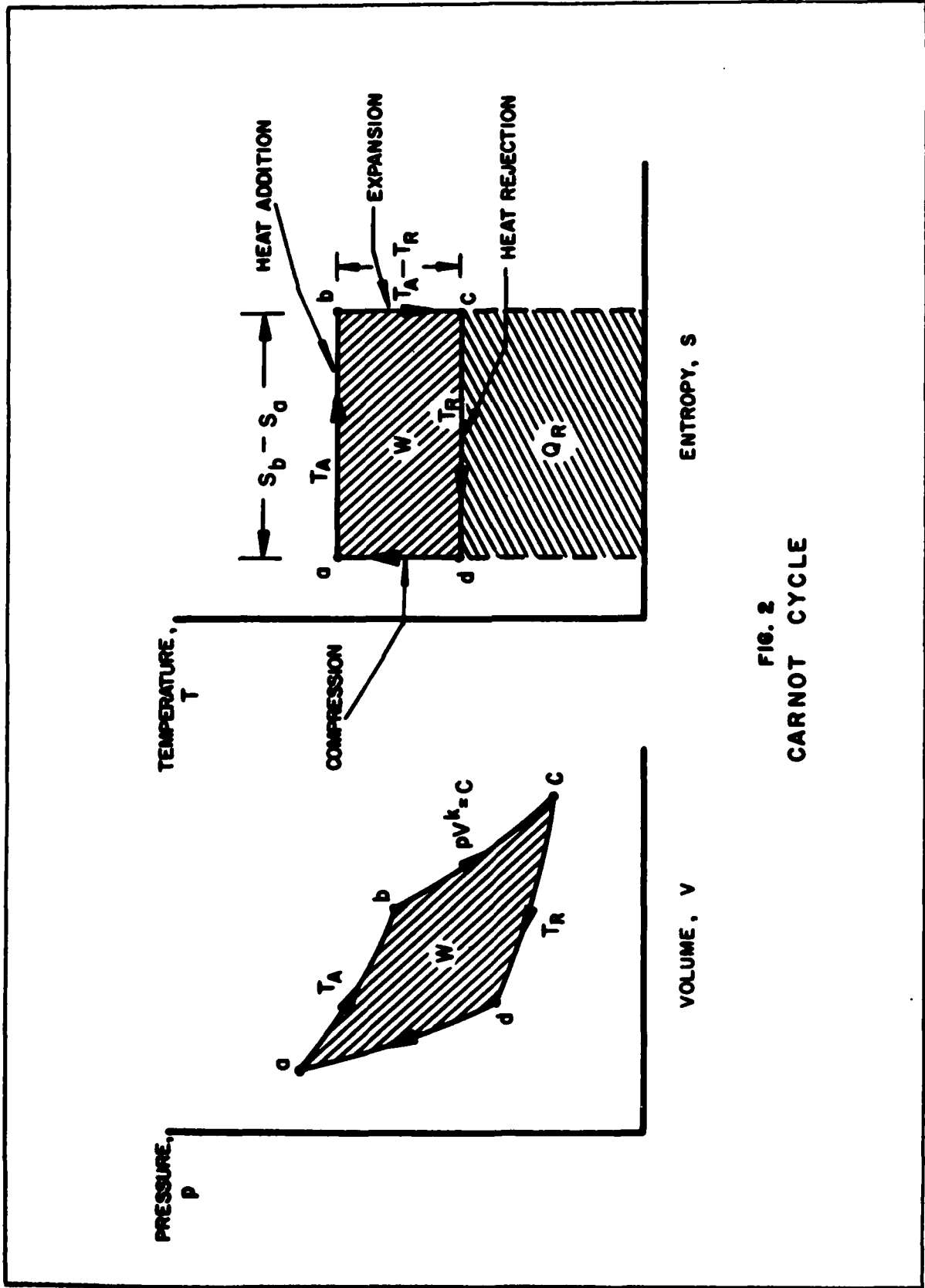


FIG. 2
CARNOT CYCLE

Rearranging Eq. (2),

$$W_C = \frac{T_A - T_R}{T_A} Q_A = \frac{T_A - T_R}{T_A} (W_C + Q_R)$$

$$W_C \left(\frac{T_A}{T_A - T_R} - 1 \right) = Q_R$$

$$W_C = \left(\frac{T_A - T_R}{T_R} \right) Q_R \quad (3)$$

The heat rejected, Q_R , is shown by the Stefan-Boltzmann equation:

$$Q_R = \sigma \epsilon A_R T_R^4 \quad (4)$$

Combining Eqs. (4) and (3), one obtains an expression for work of the cycle per unit of radiator area as a function of T_A and T_R :

$$\frac{W_C}{\sigma \epsilon A_R} = T_R^4 \left(\frac{T_A - T_R}{T_R} \right) = T_R^3 T_A - T_R^4 \quad (5)$$

For maximum work per unit radiator area, considering T_R as the only variable, $\partial W_C / \partial T_R = 0$. Therefore, to find the optimum relationship of T_R to T_A , Eq. (5) is differentiated with respect to T_R and the result is set equal to zero:

$$\frac{1}{\sigma \epsilon A_R} \frac{\partial W_C}{\partial T_R} = 3 T_R^2 T_A - 4 T_R^3 = 0$$

or

$$T_R = \frac{3}{4} T_A \quad (6)$$

Eq. (6) shows that for maximum Carnot cycle work per unit radiator area, the heat rejection temperature should be three-fourths of the heat addition temperature. This fact has been pointed out by several investigators [1, 3, 4]. Since the work has been maximized, this also means that the ratio of radiator area to cycle work has been minimized, or that the minimum radiator area occurs when the radiator temperature is three-fourths of the heat addition temperature. From Eq. (5) the following expression can be obtained for the radiator area:

$$A_R = \frac{W_c}{0.8(T_R^3 T_A - T_R^4)} \quad (7)$$

For minimum radiator area, Eqs. (6) and (7) are combined to obtain:

$$A_{R_{min}} = \frac{3W_c}{0.8T_R} \quad (8)$$

This shows that the minimum radiator area can be calculated if the power output of the cycle and the radiator temperature or the turbine inlet temperature are known. It also shows that the heat rejected is three times the power output, or that the Carnot cycle efficiency is twenty-five percent for minimum radiator area.

It should be noted that all expressions derived for the Carnot cycle are independent of the properties of the working fluid, and do not consider the inefficiencies of system components such as the pump during compression or the turbine during expansion. The analysis will now be extended to the actual Rankine cycle, to consider the non-ideal factors which are present in an actual working cycle.

b. Actual Rankine Cycle

The actual Rankine cycle is shown in Figure 3. The working fluid at point 4 is in a liquid state, and is pressurized by pumping to point 5, which corresponds to the saturation pressure at points 1 and 2. Heat is added to the liquid from point 5 until it reaches the saturation temperature at point 1. Additional heat is added as the fluid is isothermally vaporized in passing from point 1 to point 2. The vapor at point 2 is

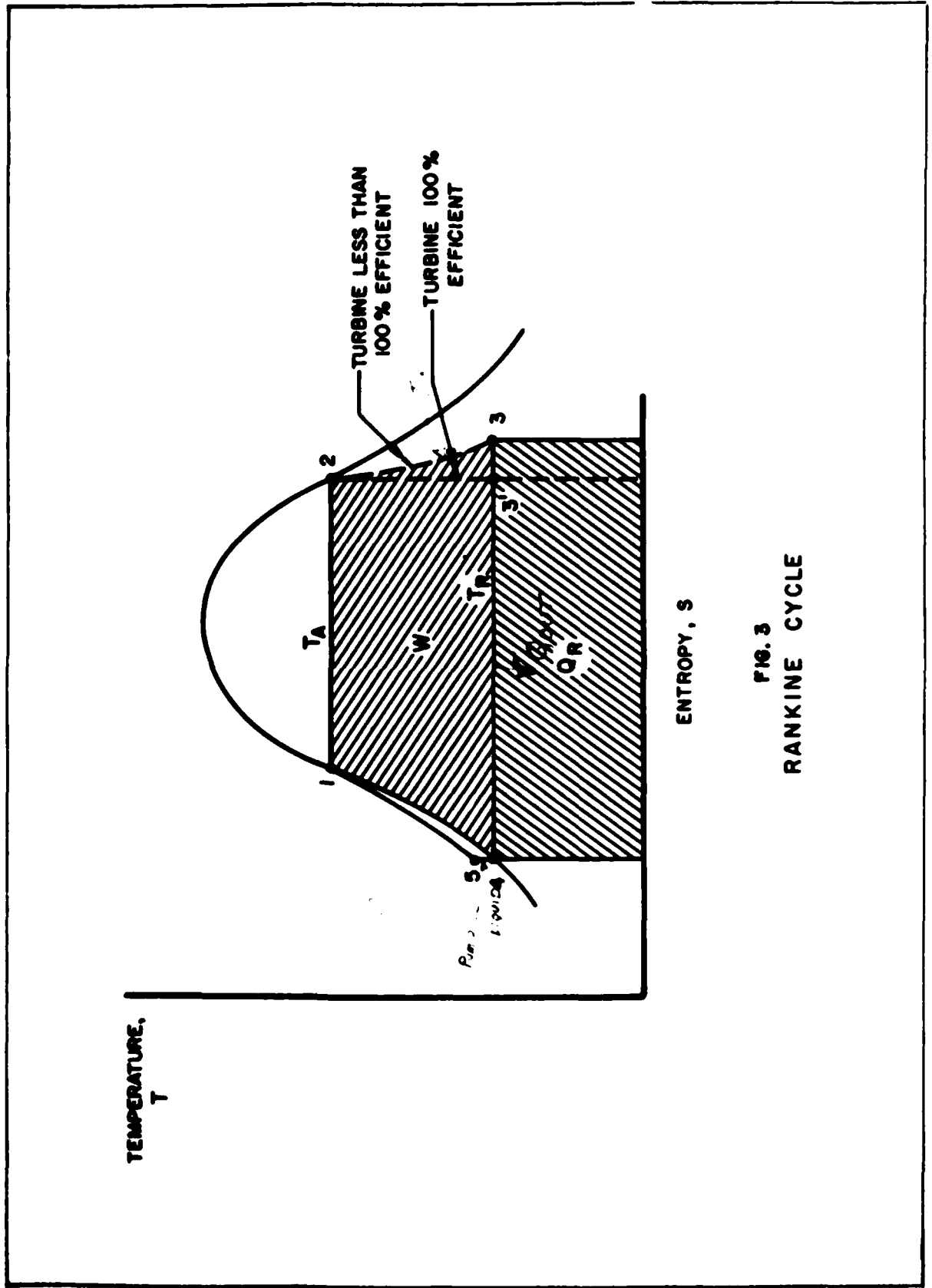


FIG. 3
RANKINE CYCLE

expanded in the turbine to point 3. If the turbine were 100 per cent efficient, the expansion would be isentropic to point 3'. The fluid is then condensed isothermally to point 4 and rejects heat during the process. At point 4, the cycle is started again. The path between points 4 and 1 is not isentropic as in the Carnot cycle because heat must be added to the fluid in a liquid state between points 5 and 1. Therefore, it is apparent that the absorption of heat by the liquid at temperatures less than the maximum temperature, T_A , decreases the efficiency to less than that of the corresponding Carnot cycle.

An actual vapor-liquid Rankine cycle differs from the ideal Rankine cycle because the actual pumping and expansion processes would be accompanied by entropy increases, and the flow processes would involve pressure losses due to fluid friction and changes in fluid momentum during phase changes. However, a preliminary cycle analysis can be made by neglecting the effects of all of these deviations except that for the turbine expansion process. Also, the pump work may be neglected without serious results. Therefore, in the following analysis, the actual Rankine cycle will be considered as the process 1-2-3-4-1 illustrated in Figure 3.

Referring to Figure 3, the heat added to the working fluid may be expressed as the heat necessary to raise the temperature of the liquid from T_D to T_A , plus the heat necessary to completely vaporize the fluid. In other words, it is the change in enthalpy between point 4 and point 2:

$$Q_A = h_2 - h_4 \quad (9)$$

The heat rejected by the working fluid is that heat which is released during the condensation of the wet turbine exhaust vapor at point 3 to the saturated liquid at point 4, i.e.:

$$Q_R = h_3 - h_4 \quad (10)$$

The work of the actual Rankine cycle, W_R , is the difference between the heat added and the heat rejected:

$$W_R = Q_A - Q_R = h_2 - h_3 \quad (11)$$

Referring to Figure 3, the work is the difference in enthalpy between point 2 and point 3, or the change in enthalpy when the working fluid undergoes expansion in the turbine. If the turbine were 100 percent efficient, the expansion would be isentropic, i.e., the work would be the difference in enthalpy between point 2 and point 3'. But because the actual turbine is less than 100 percent efficient, the expansion takes place with an increase in entropy, to point 3. Thus, the work of the cycle may also be expressed in the following manner to take into account the turbine efficiency η_t :

$$W_r = \eta_t (h_2 - h_3) \quad (12)$$

The efficiency of the actual Rankine cycle is the ratio of the work of the cycle to the heat added to the cycle:

$$\eta_r = \frac{h_2 - h_3}{h_2 - h_4} = \frac{\eta_t (h_2 - h_3')}{h_2 - h_4} \quad (13)$$

To obtain a picture of the differences in the efficiencies of the Carnot cycle, the ideal Rankine cycle (turbine 100 percent efficient), and the actual Rankine cycle (turbine less than 100 percent efficient), Figure 4 has been prepared. This figure is based upon the use of potassium as the working fluid, with a turbine inlet temperature of 2100°R, and varying radiator temperatures. For the actual Rankine cycle, a turbine efficiency of 85 percent was assumed.

At this time, it is convenient to introduce the work factor, k , which may be defined as

$$k = \frac{\eta_r}{\eta_c} = \frac{W_r}{W_c} \quad (14)$$

In other words, the work factor, k , is the ratio of efficiency, and of the work, of the actual Rankine cycle to that of the Carnot cycle. The work factor will be useful in determining the optimum temperature ratios and minimum radiator area for the actual Rankine cycle.

The work of the actual Rankine cycle may also be expressed as the product of the heat added and the cycle

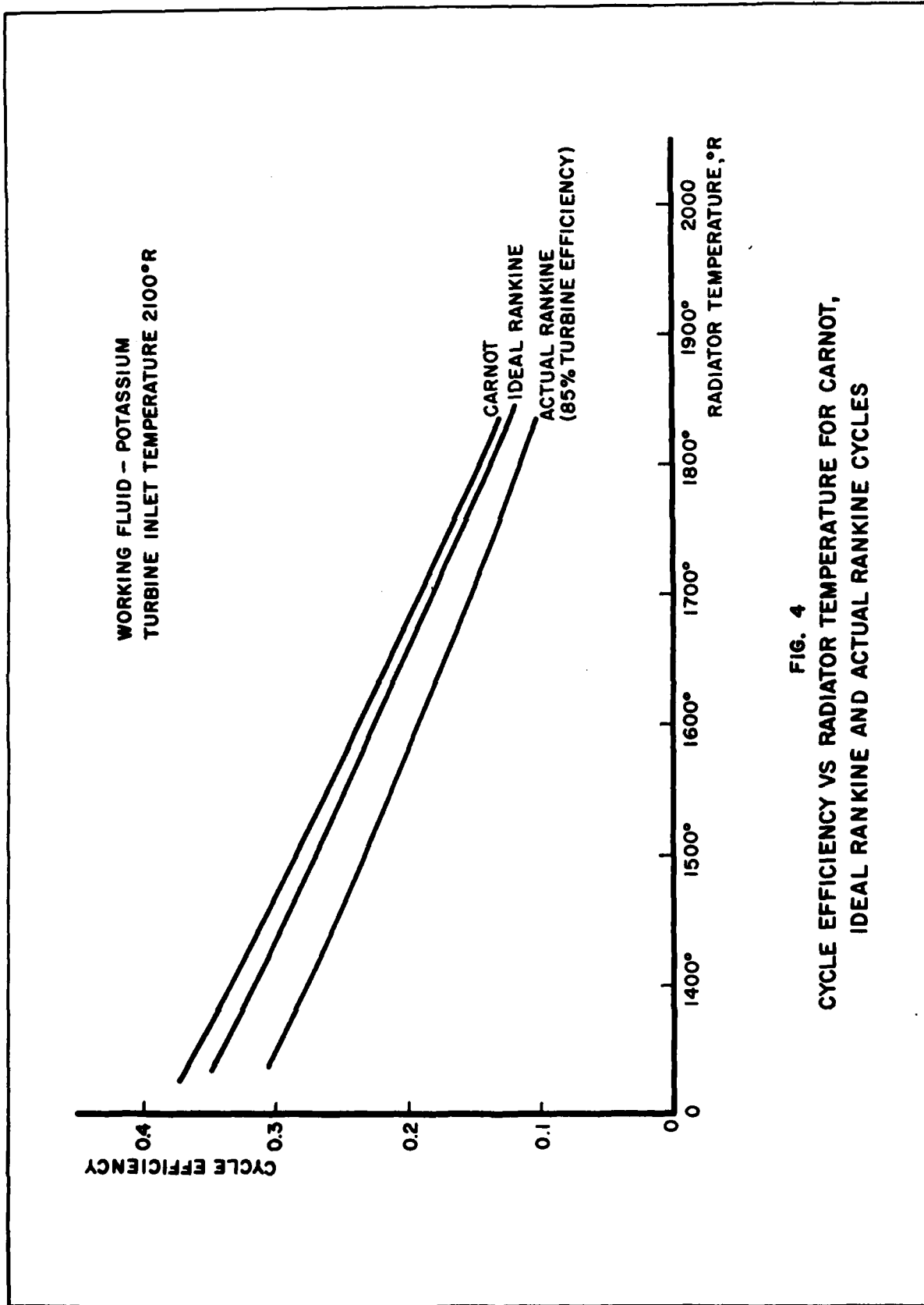


FIG. 4
CYCLE EFFICIENCY VS RADIATOR TEMPERATURE FOR CARNOT,
IDEAL RANKINE AND ACTUAL RANKINE CYCLES

efficiency:

$$W_r = Q_A \eta_r \quad (15)$$

Combining Eqs. (11) and (15),

$$Q_A - Q_R = Q_A \eta_r$$

or

$$Q_A (1 - \eta_r) = Q_R \quad (16)$$

The heat rejected by the radiator is:

$$Q_R = \sigma \epsilon A_R T_R^4 \quad (4)$$

which may be combined with Eq. (16) to obtain

$$Q_A (1 - \eta_r) = \sigma \epsilon A_R T_R^4$$

or

$$Q_A = \frac{\sigma \epsilon A_R T_R^4}{1 - \eta_r} \quad (17)$$

Combining Eqs. (1) and (14), one obtains

$$\eta_r = k \eta_c = k \left(\frac{T_A - T_R}{T_A} \right) \quad (18)$$

which may be used in Eq. (17) to obtain the following expression for the heat added to the actual Rankine cycle:

$$Q_A = \frac{\sigma \epsilon A_R T_R^4}{1 - k \left(\frac{T_A - T_R}{T_A} \right)} \quad (19)$$

Since the work of the actual Rankine cycle is expressed by Eq. (15), it may be combined with Eq. (19) to obtain:

$$W_r = \eta_r \frac{\sigma \epsilon A_R T_R^4}{1 - k \left(\frac{T_A - T_R}{T_A} \right)} \quad (20)$$

Using the value of η_r from Eq. (18) in combination with Eq. (20), the work of the actual Rankine cycle per unit radiator area may be finally expressed by:

$$\begin{aligned} \frac{W_r}{\sigma \epsilon A_R} &= k \left(\frac{T_A - T_R}{T_A} \right) \frac{T_R^4}{1 - k \left(\frac{T_A - T_R}{T_A} \right)} \\ &= \frac{k T_R^4}{\frac{T_A}{T_A - T_R} - k} \end{aligned} \quad (21)$$

As in the case of the Carnot cycle, the work of the actual Rankine cycle per unit radiator area can be optimized by differentiating Eq. (21) with respect to T_R and setting the result equal to zero, as shown in the following steps:

$$\begin{aligned} W_r &= \sigma \epsilon A_R k \frac{T_R^4}{\frac{T_A}{T_A - T_R} - k} \\ \frac{\partial W_r}{\partial T_R} &= (\sigma \epsilon A_R k) \frac{4 T_R^3 \left(\frac{T_A}{T_A - T_R} - k \right) - T_R^4 \frac{T_A}{(T_A - T_R)^2}}{\left(\frac{T_A}{T_A - T_R} - k \right)^2} = 0 \end{aligned}$$

$$4 \left(\frac{T_A}{T_A - T_R} - k \right) = T_R \frac{T_A}{(T_A - T_R)^2}$$

$$4 k T_R^2 - T_R T_A (8k - 5) - 4 T_A^2 (1-k) = 0$$

Therefore,

$$T_R = \frac{T_A (8k - 5) \pm \sqrt{T_A^2 (8k - 5)^2 + 64 k T_A^2 (1-k)}}{8k}$$

Rearranging, and disregarding the minus root, which does not have a physical meaning:

$$\frac{T_R}{T_A} = 1 - \frac{5}{8k} + \frac{1}{8k} \sqrt{25 - 16k} \quad (22)$$

This equation expresses the relationship between the radiator temperature and the heat addition temperature for the case of optimum work and minimum radiator area of the actual Rankine cycle. For the Carnot cycle, $k = 1$, and it is interesting to note that $T_R = 3/4 T_A$, which is the same value shown by Eq. (6).

It is enlightening to visualize the effect that varying values of the work factor, k , have upon the optimum temperature ratio, T_R/T_A . Figure 5 illustrates the relationship between k and T_R/T_A when values of k from 0.3 to 1.0 are inserted in Eq. (22). It may be seen that the value of T_R/T_A lies between 0.75 and 0.80, and does not differ too greatly from 0.75, which is the value determined for optimum Carnot cycle performance. This fact has been pointed out by Electro-Optical Systems, Inc. [5]. Thus, it may be concluded that the radiator temperature for the actual Rankine cycle will always be approximately three-fourths of the turbine inlet temperature.

Equation (21) can be rearranged to provide an expression for the radiator area of the actual Rankine cycle:

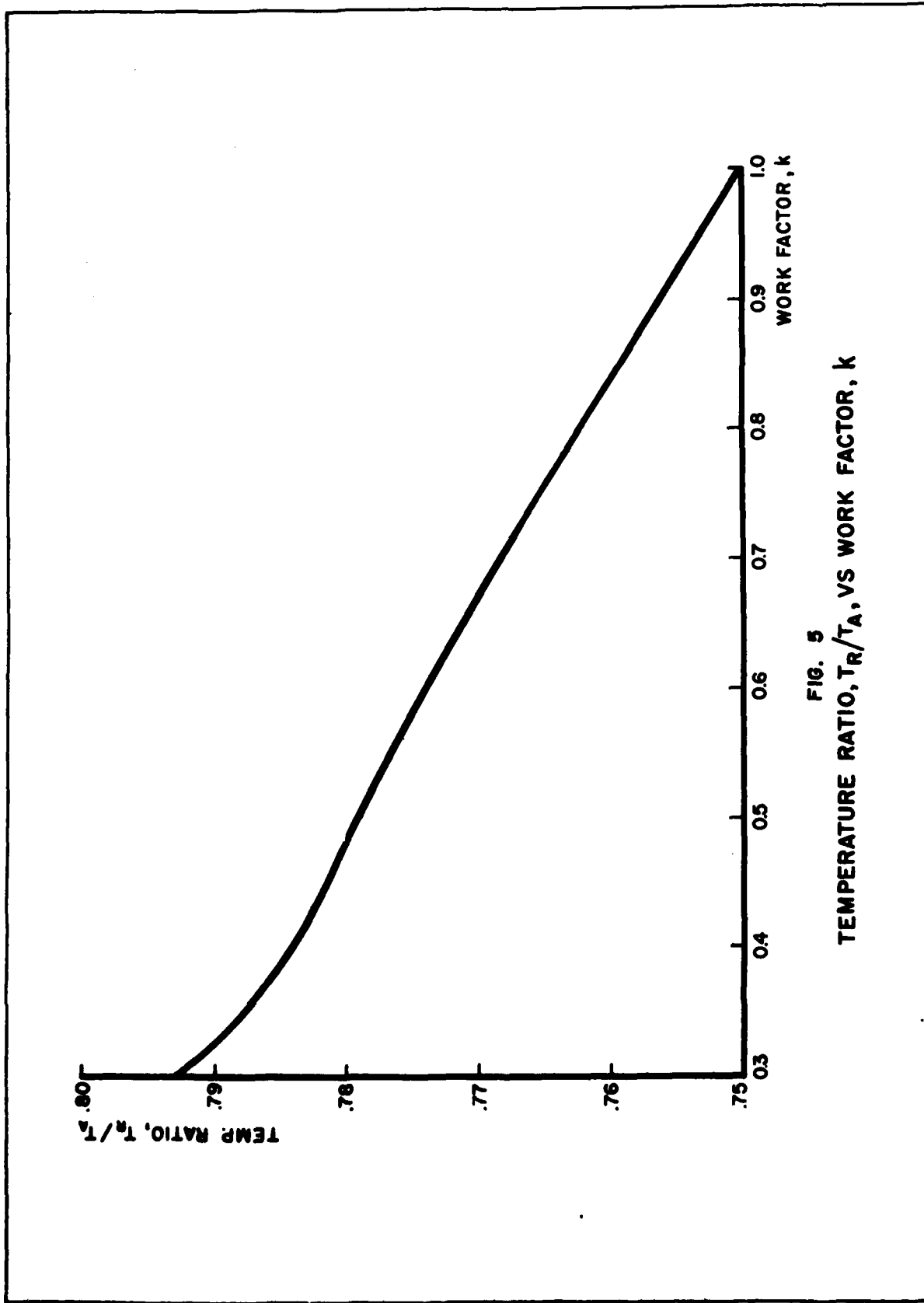


FIG. 5
TEMPERATURE RATIO, T_R/T_A , VS WORK FACTOR, k

$$A_R = \frac{W_r \left(\frac{T_A}{T_A - T_R} - k \right)}{\sigma \epsilon k T_R^4} \quad (23)$$

Thus, with Eq. (22), it is possible to determine the optimum radiator temperature for any given value of T_A , and using these temperature values, to determine the minimum radiator area by using Eq. (23).

The turbine inlet temperature of the working fluid has a great effect upon the radiator area, as may be expected. Since the heat radiated varies as the fourth power of the radiator temperature, any increase in turbine inlet temperature will result in an increased radiator temperature, and a consequent substantial increase in the heat radiated. Figure 6 indicates the decrease in radiator area for progressively higher turbine inlet temperatures. For this figure, the actual Rankine cycle was used, with a system power output of 1 megawatt, a turbine efficiency of 85 percent, and potassium as the working fluid. It should be noted that for minimum radiator area, the radiator temperature is always approximately three-fourths of the turbine inlet temperature, as previously determined.

Thus far, the thermodynamics of the ideal Carnot cycle and the actual Rankine cycle have been investigated, the differences in efficiencies of the cycles have been illustrated, expressions have been determined for the optimum relationship between turbine inlet temperature and radiator temperature and for the minimum radiator area, and the effect of increased temperatures upon radiator area has been illustrated. In the next section, suitable working fluids will be evaluated.

3. WORKING FLUIDS

Proper selection of the working fluid for the system is of utmost importance. The properties of the fluid will affect the efficiency of the cycle, the weight of the system, and the performance temperature. The primary functions of the working fluid are to absorb heat from the nuclear reactor heat source, provide driving force for the turbine, and carry waste heat from the turbine to the heat rejection system. In addition, it may provide lubrication for moving parts in the system.

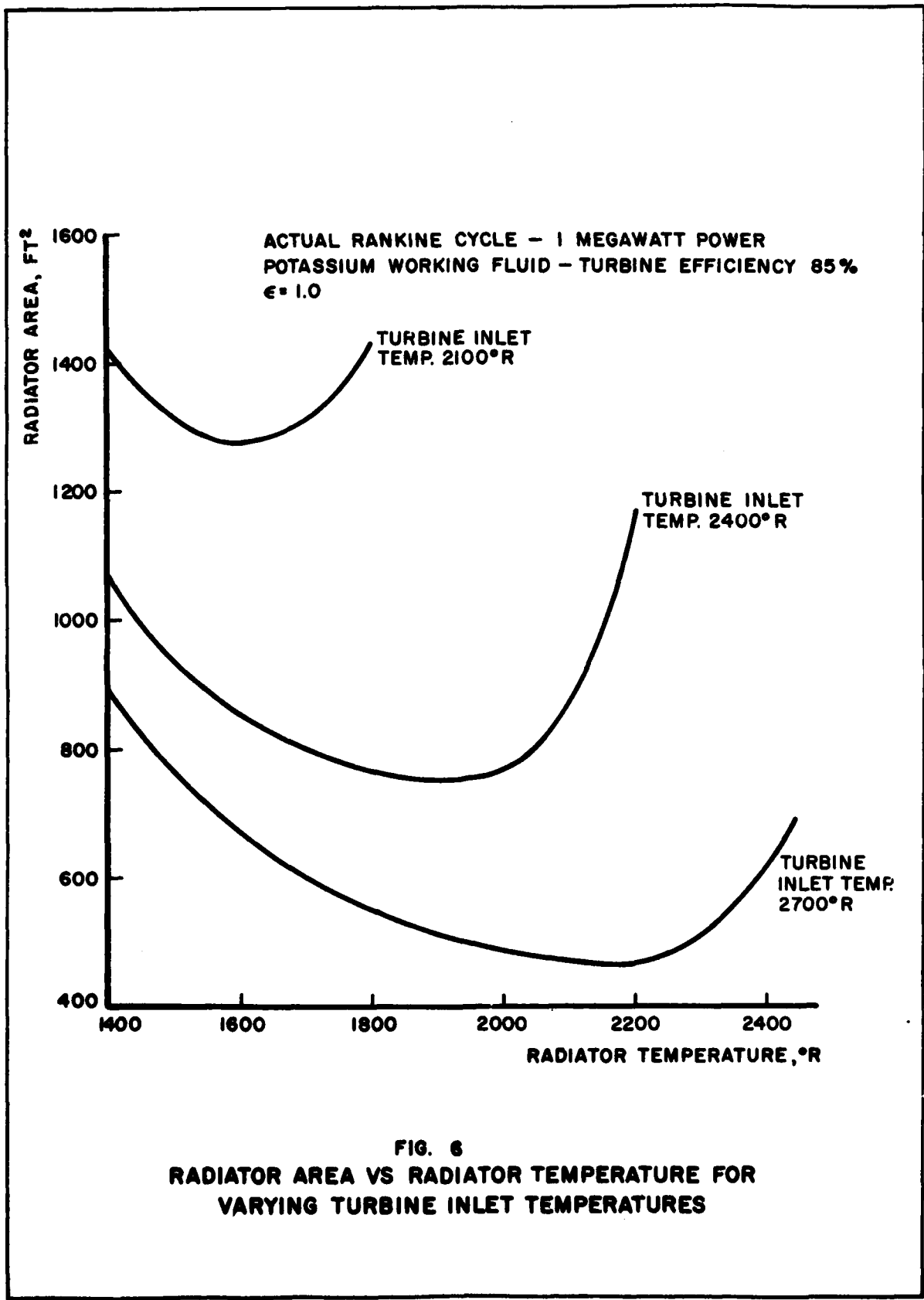


FIG. 6
 RADIATOR AREA VS RADIATOR TEMPERATURE FOR
 VARYING TURBINE INLET TEMPERATURES

Working fluids may be elements, alloys or compounds. The elements are more favorable than the alloys or compounds because of their greater stability during long-term operation. Alloys and compounds may decompose or change properties when undergoing boiling or during high temperature operation, or when subjected to nuclear radiation. Therefore, in this report, consideration will be given only to elements as possible working fluids.

The following physical properties of the working fluid are of interest when the fluid is considered for use in a turbine and radiator:

- (1) Melting point — low melting points are desirable for ease of start-up.
- (2) Boiling point — boiling points should be low enough to permit condensation at reasonable pressures without requiring heavy structures.
- (3) Vapor pressure — vapor pressure should be low enough at operating temperatures to avoid a requirement for heavy plumbing.
- (4) Specific volume of vapor — specific volumes should be low, or conversely, densities should be high, to minimize the sizes of vapor passages.
- (5) Density of liquid — the density of the liquid should be low to reduce the weight of the fluid inventory.
- (6) Viscosity — the viscosity of the fluid should be low to reduce pressure drops in flow passages.

In addition to favorable physical properties as just described, the working fluid should also have favorable heat transfer properties, such as:

- (1) Thermal conductivity — the thermal conductivity of the fluid should be high to assure adequate heat transfer with a minimum area.
- (2) Specific heat — the specific heat of the fluid should be high to minimize the fluid inventory and structure.

- (3) Latent heat of vaporization — the latent heat of vaporization should be high to minimize the fluid inventory and structure.

For the power cycle as considered in this paper, the following properties of the working fluid are also of interest:

- (1) Neutron absorption cross section — the neutron absorption cross section should be low to assure reliable long-term operation with the nuclear reactor heat source.
- (2) Corrosiveness — the fluid should be as non-corrosive as possible to assure compatibility with available structural materials.
- (3) Long-time stability under high temperatures and nuclear radiation — the fluid must not lose its properties during extended exposure to nuclear radiation and continued high temperatures.

A number of firms have investigated fluids suitable for power cycles and cooling systems in space applications. One of the most recent studies was by Southwest Research Institute, under sponsorship of the Wright Air Development Center. Their technical report by Weatherford, Tyler and Ku [6] states that several considerations are necessary in selecting a suitable fluid:

"As design temperatures increase in the future, it may be necessary to consider less volatile coolants than alkali metals in order to avoid excessive Rankine cycle pressures. With this thought in mind, (the following table) presents a summary of selected metals with boiling points ranging from that of mercury at less than 700°F to that of tin at nearly 5000°F. Two criteria have been used for selecting the specified metals. One is that the melting point is less than 640°F so that start-up does not present unnecessary problems. The other criterion is that the temperature range in which metal is liquid at atmospheric pressure is greater than 60 percent of the absolute boiling temperature in order that cycle temperatures and, hence, cycle efficiencies will not be unnecessarily restricted by the avoidance of solid-phase formation or excessive vapor pressures. It should be noted that the described selection criteria ruled out consideration of aluminum, cadmium, zinc, magnesium, and antimony which have been considered previously as potential liquid-metal coolants.

Metal	Symbol	Normal Boiling Point, °R	Melting Point, °R	Melting Point-Boiling Point Ratio
Mercury	Hg	1134	422	0.37
Cesium	Cs	1720	543	0.32
Rubidium	Rb	1730	562	0.32
Potassium	K	1860	606	0.32
Sodium	Na	2093	668	0.32
Lithium	Li	2897	817	0.28
Thallium	Tl	3132	1039	0.33
Bismuth	Bi	3298	981	0.30
Lead	Pb	3643	1082	0.30
Indium	In	4176	772	0.27
Gallium	Ga	4518	545	0.12
Tin	Sn	5328	909	0.17 ."

The discussion thus far in this section indicates that the working fluid should preferably be an element, and that liquid metals are attractive. In addition to the liquid metals, sulfur and phosphorus are in the correct temperature range for application in heat rejection systems. However, very little is known about the corrosiveness or material compatibility of sulfur and phosphorus at elevated temperatures, except for some data showing that sulfur is compatible with selected ceramic materials up to 1600°F [6]. Therefore, sulfur and phosphorus will not be considered further in this paper.

As a first step in selecting suitable working fluids, an upper temperature limit can be imposed. It may be reasonably expected that approximately 2500°F will be the temperature limitation of structural materials within the next decade or so. Using 2500°F as an upper limit, and selecting from the table just shown, the liquid metals then suitable for a working fluid are mercury, cesium, rubidium, potassium, sodium and lithium.

As a second step in choosing the working fluid, consideration is given to the vapor pressures of the six suitable liquid metals. Figure 7 shows the vapor pressures plotted against the temperature. This figure may be used to impose further restrictions upon the fluid. A lower temperature limit of 600°F will be set to assure efficient operation of the cycle and of the radiator. An upper temperature limit of 2500°F has already been selected. A lower pressure limit of 3 psia will be selected to avoid bulky and heavy flow passages due to the associated high specific volumes. An upper pressure limit of several hundred psia will be selected to avoid heavy pressurized structures.

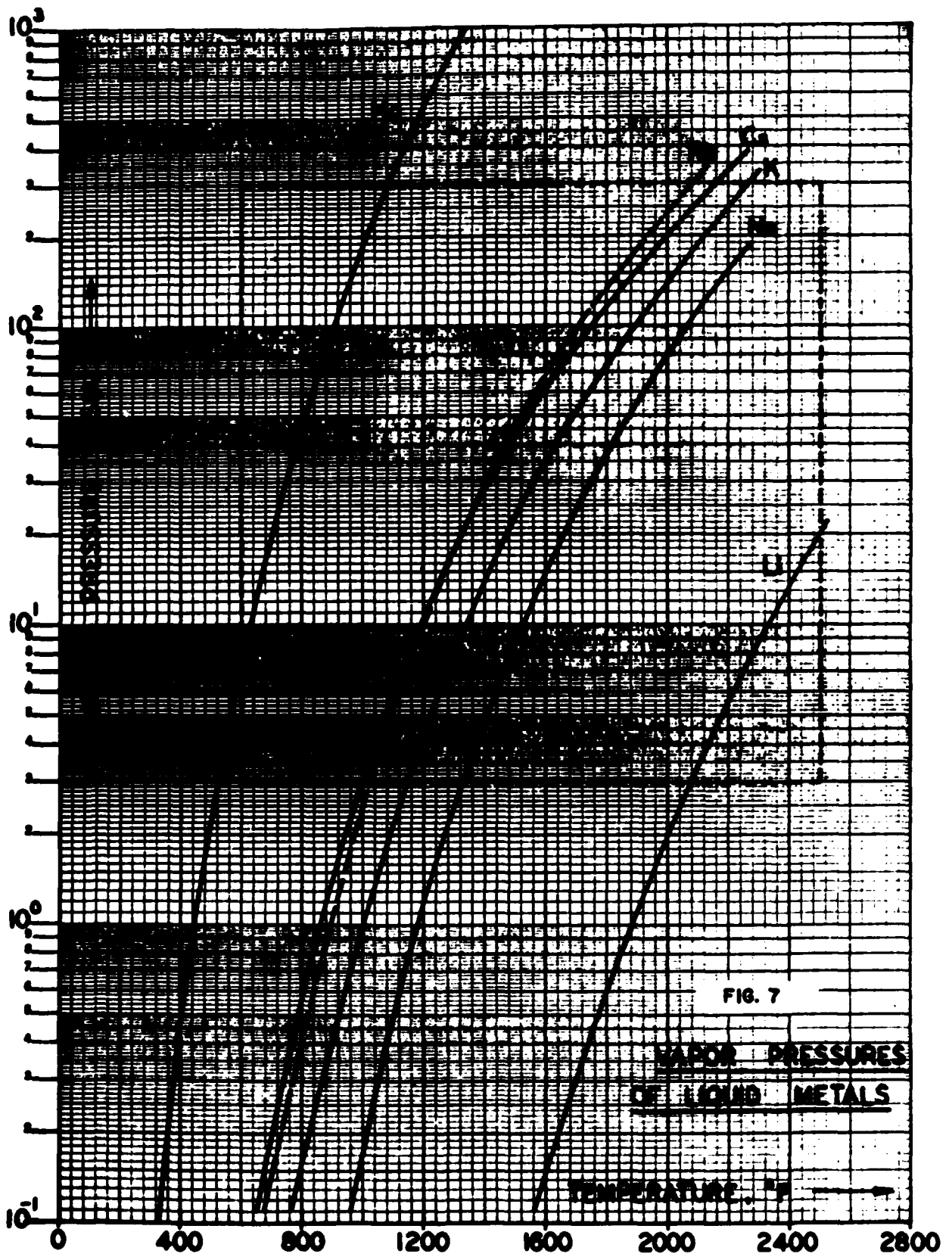


FIG. 7

VAPOR PRESSURES
OF LIQUID METALS

TEMPERATURE, °F

When these limits are shown on Figure 7, it becomes apparent that the most attractive fluids are rubidium, cesium, potassium, and sodium. Lithium appears to be more attractive for higher temperature systems, and mercury for lower temperature systems.

A third step in narrowing the selection of the working fluid is to consider the neutron absorption cross sections of the six liquid metals. The thermal neutron (2200 m/e) absorption cross sections of the naturally occurring elements are given by [6] as follows:

Mercury	380	±	20	barns
Cesium	29	±	1.5	barns
Rubidium	0.70	±	0.07	barns
Potassium	1.97	±	0.06	barns
Sodium	0.505	±	0.010	barns
Lithium	71.0	±	1.0	barns

The high neutron absorption cross sections for mercury, cesium, and lithium make them unsuitable for use in a vapor-condensing cycle utilizing a nuclear reactor heat source. An isotope of mercury, Hg^{200} , has an absorption cross section of 0.43 ± 0.10 barns, and thus could be considered for use in a nuclear reactor if its other properties were more attractive than rubidium, potassium or sodium. Recognizing that mercury, cesium, and lithium are not well suited for the nuclear reactor-thermal system considered here because of their high cross sections, the remaining fluids are rubidium, potassium, and sodium.

The physical and thermal properties of rubidium, potassium, and sodium are shown in Table 1. Comparing the properties of the fluids, several differences are significant. The density of rubidium vapor at the boiling point is approximately twice that of potassium and approximately four times that of sodium. This would indicate that smaller vapor passages would be required for rubidium. However, the latent heat of vaporization of rubidium is less than that of potassium and sodium, so for a given power rating, a greater mass of rubidium must be condensed, thus offsetting its apparent advantage of higher vapor density. The lower viscosity of potassium vapor makes potassium appear advantageous. The higher specific heat and higher thermal conductivity of sodium makes that fluid attractive.

The difference in boiling points for the three fluids require different operating temperatures to assure optimum cycle

TABLE 1

PHYSICAL AND THERMAL PROPERTIES OF RUBIDIUM, POTASSIUM AND SODIUM*

	<u>Rubidium</u>	<u>Potassium</u>	<u>Sodium</u>
Atomic Weight	85.48	39.10	22.997
Melting Point, °F	102	145.8	208
Boiling Point, °F	1270	1400	1618
Critical Point, psia	2790	1500+ 735	5042
	(3032 °F)	(3095+540 °F)	(3632 °F)
Density of Liquid, lb/ft ³	82.15	41.38	46.4
Density of Vapor, lb/ft ³	0.060	0.0305	0.0165
Viscosity of Liquid, lb/ft hr	0.363	0.323	0.37
Viscosity of Vapor, lb/ft hr	0.0407	0.0235	0.0313
Surface Tension, lb/ft	0.0034	0.0059 (212 °F)	0.01306
Thermal Conductivity of Liquid, BTU/hr ft °F	11.8	18.0	30.1
Thermal Conductivity of Vapor, BTU/hr ft °F	0.00354	0.0045	0.0083
Specific Heat of Liquid, BTU/lb °F	0.0877	0.1868	0.305
Specific Heat of Vapor, BTU/lb °F	0.0579	0.1267	0.214
Latent Heat of Fusion, BTU/lb	11.79	25.5	48.7
Latent Heat of Vaporization, BTU/lb	347.5	851	1609

* Data from Reference [6]

efficiency and optimum radiator area for each fluid. Thus, it may be seen that it is difficult to select the most suitable working fluid for the system described herein without making a complete cycle performance analysis for each of the fluids, and then comparing the analyses. Such a procedure is beyond the scope of this report.

Potassium has physical and thermodynamic properties generally between those of rubidium and sodium, so may be considered to be a reasonable choice. Also, the properties of potassium are well known, which will enhance the accuracy of thermodynamic calculations. Potassium is commercially available, and thus has an advantage over rubidium.

Reference [6] contains figures for the foregoing fluids showing the vapor pressure, liquid density, vapor density, liquid viscosity, vapor viscosity, and materials compatibility, as well as a Mollier diagram for each fluid. In addition, Ref. [6] contains tables showing the physical, thermal, and thermodynamic properties of the fluids, and should be consulted if further data is desired.

REFERENCES

1. D. Mackay: **Powerplant Heat Cycles for Space Vehicles** (paper presented at the Institute of Aeronautical Sciences Summer Meeting, Los Angeles, California, 16-19 June 1959).
2. V. Faires: **Applied Thermodynamics**, The MacMillan Company, New York, 1948.
3. E. Pitkin: **Optimum Radiator Temperature for Space Power Systems**, ARS Journal, Vol. 29, No. 8, p. 596, August 1959.
4. **Study of Heat Rejection in Space**, Interim Report 250-IR-1, Electro-Optical Systems, Inc., Pasadena, Calif., July 1959.
5. **A Proposal for the Analysis and Development of a Space Heat Rejection System and its Optimum Integration into a Space Vehicle**, Electro-Optical Systems, Inc., Pasadena, Calif., September 1958.
6. W. Weatherford, Jr., J. Tyler, P. M. Ku: **Properties of Inorganic Working Fluids and Coolants for Space Applications**, Southwest Research Institute, WADC Tech. Rpt. 59-598, 1959.

DISTRIBUTION

GEORGE C. MARSHALL SPACE FLIGHT CENTER

**M-DIR
M-DEP-R&D**

M-FUT-DIR

M-MS-I

**M-G&C-DIR
M-G&C-E
M-G&C-M
M-G&C-A
M-G&C-R**

M-LOD-D (Mr. von Tiesenhausen)

**M-S&M-F (Mr. Barker)
M-S&M-FE (Mr. R. Callaway)
M-S&M-FE (Mr. W. Jordan)
M-S&M-E
M-S&M-S
M-S&M-SR (Mr. Blumrich)
M-S&M-TSM (Dr. Kuettner)**

**M-RP-DIR
M-RP-P (Dr. Lundquist)
M-RP-T (Mr. Heller)
M-RP-T (Dr. Schocken)
M-RP-T (Mr. Jones)
M-RP-T (Mr. Snoddy)
M-RP-N (Dr. Shelton)
M-RP-N (Dr. Weber)
M-RP-N (Mr. Seitz)**

**M-RP-S (Mr. Thompson)
M-RP-R (Mr. Miles)
M-RP-R (Mr. Downey)
M-RP-TS (Mr. Bucher)(6)
M-RP-PCA (Mrs. Christopher (10))**

NASA HEADQUARTERS

Dr. W. C. Cooley	LP
Dr. H. Harrison	LP
Mr. H. Finger	LP
Dr. F. Schulman	LP
Mr. A. von Doenhoff	DL
Mr. H. Rothen	RPP

LEWIS RESEARCH CENTER

Dr. John Evvard
Mr. Henry Slone
Mr. Richard P. Goye

LANGLEY RESEARCH CENTER

Mr. Joseph Hallisy, Jr.

JET PROPULSION LABORATORY

Mr. Herman Bank